Proton Motion in Aliphatic Nylons from Neutron Scattering

A. Xenopoulos, B. Wunderlich,* and A. H. Narten†

Chemistry Division, Oak Ridge National Laboratory, Oak Ridge, Tennessee 37831-6197, and Department of Chemistry, University of Tennessee, Knoxville, Tennessee 37996-1600

Received July 9, 1992; Revised Manuscript Received December 18, 1992

ABSTRACT: Quasielastic neutron scattering studies on samples of aliphatic Nylons with different crystallinities show that at temperatures below the calorimetric glass transition (310–330 K) the scattering is elastic, indicating that the protons, and hence the methylene groups to which they are bound, undergo only small-amplitude vibrations about their equilibrium positions. As the temperature increases, the elastic scattering decreases gradually, to be replaced by quasielastic components. The decrease in elastic intensity occurs not only in the amorphous regions but also in the crystals. In Nylon 6.6 at temperatures 40 K below melting there is practically no elastic scattering intensity left. The experimental observations are compared with NMR and thermal analysis work, that has also indicated large-amplitude motion in Nylon crystals, and are discussed in reference to molecular dynamics simulations on the hexagonal phase of paraffins.

Introduction

Aliphatic Nylons consist of methylene sequences separated by hydrogen-bonded amide groups.[1,2] The methylene segments are thus anchored on both sides but are allowed to move otherwise independently. The possible constrained mobility of methylene groups in Nylons and the stability of the crystal to high temperatures have prompted our work on the dynamics of Nylons.

Aliphatic Nylons are usually semicrystalline, with crystallinities ranging typically from 30 to 70%. The glass transition temperature (T_g) of semicrystalline Nylons is in the range 310–330 K, as determined by differential scanning calorimetry (DSC). At this temperature, cooperative main-chain mobility begins in the amorphous part of the polymer. A broad transition, named after Brill,[3] occurs in the crystals of Nylon 6.6 at about 450–490 K and is accompanied by changes in the mechanical properties. Crystallographically, a gradual crystal transformation from the room-temperature triclinic structure to a high-temperature pseudohexagonal one occurs in this temperature range.[4] The increase in symmetry at the Brill transition is accompanied by a marked increase in segmental mobility of the methylene groups, as was seen already from early NMR studies.[5] The hydrogen bonds remain, however, intact up to the melting temperature, as was seen by infrared spectroscopy.[6]

The segmental dynamics in both the crystalline[7] and the amorphous[8] portions of Nylon 6.6 were recently studied by solid-state deuterium NMR using selectively deuterated samples and molecular dynamics simulations.[9] It was found that in the crystalline part the N–D and C–D groups undergo spatially-heterogeneous, librational motion both below and above the Brill transition. At 500 K the amplitude of the C–D motion in the crystals becomes very large, reaching an angle of 60°, similar for all methylenes. The correlation times are on the average 4×10^{-11} s for all C–D groups. The librational motion of the N–D bonds is more restricted, with a correlation time of 3×10^{-10} s, and the hydrogen bonds do not break. In the amorphous part, limited librations and internal rotations are already possible below T_g, while above T_g both N–D and C–D sites perform nearly isotropic motion.

A detailed thermal analysis study on a series of aliphatic Nylons[10-12] indicated an increase in heat capacity above the glass transition temperature beyond that expected for vibrating crystals and a given amorphous fraction. This gradual increase in heat capacity was interpreted by comparison with polyethylene to be a manifestation of conformational disorder[13] resulting from the potential energy contribution of large-amplitude motion.[14] In Nylon 6.6 the melting temperature (574 K)[15] is considerably higher than in polyethylene (414.6 K), and one may expect even larger amounts of conformational disorder for the methylene groups in the vicinity of the melting temperature.

Incoherent quasielastic neutron scattering (IQNS)[16] is a dynamic method that can give direct spatial information on proton dynamics at faster than nanosecond time scales, depending on the energy resolution of the instrument. For hydrogenous systems, the scattering of neutrons is dominated by the incoherent cross section of the protons. Incoherent scattering contains no interference effects between different nuclei, only between neutrons scattered from the same nucleus, but at different times. The scattering is thus determined by the space–time trajectories of the protons. The quantity accessible from neutron scattering is the function $S(k,\omega)$, which measures the probability that energy, $\hbar\omega$, is transferred to the proton with the momentum change $\hbar k$ to the neutron.[17] Note that, for the macroscopically isotropic samples studied here, only the magnitude of the wave vector $\mathbf{k}$ needs to be considered.

When there is no energy transfer, the scattering is said to be elastic. Elastic scattering occurs when the protons vibrate near their equilibrium positions, as in a solid at low temperatures. When the energy transfer is small in magnitude (less than a few millielectronvolts), quasielastic scattering is said to occur. This type of scattering is the result of the interaction of the neutrons with protons undergoing random motions, and it therefore gives information about translational and rotational diffusion in solids and liquids. For small values of the momentum transfer k, the dynamic coupling between single particle diffusion and other contributions can often be neglected. In these cases the incoherent scattering function can be separated into an elastic and a quasielastic contribution.

$$S_{inc}(k,\omega) = S_{el}(k) + S_{qe}(k,\omega) \quad (1)$$

The scattering function is further modulated by the Debye–Waller factor, $\exp(-u^2k^2)$, that describes the attenuation of the scattering intensity due to oscillatory motion of the protons, defined by a mean-square amplitude u^2.

† Deceased.

0024-9297/93/2226-1576$04.00/0

The elastic incoherent structure factor (EISF) $A(k)$ is equal to $S_{el}/[S_{el} + S_{qe}]$. It is a direct measure of the time-averaged spatial distribution of the protons and contains all geometrical information about the diffusive process. It shows characteristic damped oscillations with a phase factor kr, where r is an average distance characteristic of the diffusive process.[18] For restricted motions, the loss of orientational correlation is incomplete and leads to plateau values different from zero, which can also be used to distinguish different types of motion. For rotational jumps between n equivalent points j on a circle of radius r the expression for a powder sample is[19]

$$A(k) = \frac{1}{n}\sum_{j=1}^{n} f\{2kr \sin(\pi j/n)\} \quad (2)$$

with $f(x) = [\sin(x)]/x$. For continuous rotational diffusion on a sphere of radius r the EISF would be

$$A(k) = [\sin^2(kr)]/(kr)^2 \quad (3)$$

The quasielastic broadening $S_{qe}(k,\omega)$ determines the time scale of the diffusive motions, i.e. the finite probability that the protons have moved out of the original measurement space of the neutron, determined by its wavelength. Since the decay of particle density is frequently exponential, it leads to a Lorentzian component centered about the elastic position. The quasielastic broadening then takes the form

$$S_{qe}(k,\omega) = \{1 - A(k)\}\frac{1}{\pi}\frac{\tau}{1 + \omega^2\tau^2} \quad (4)$$

with τ being a correlation time characteristic of the diffusive process.

Quasielastic scattering has been used extensively to study dynamics in dense systems, but semicrystalline polymers have received less attention.[20] In this paper we present IQNS results on two samples of Nylon 6.6, with different crystallinities, and one sample of Nylon 6, at different temperatures. It is shown that as the temperature increases, dramatic changes in the IQNS signal occur, signifying corresponding changes in the proton motions in both the amorphous and crystalline regions.

Experimental Section

Samples. Nylon 6.6 (approximate molecular mass 15 000–20 000 amu) was obtained from the DuPont Co. in pellet form. It has a melting temperature T_m = 540 K and a glass transition temperature T_g = 323 K. For the solution-crystallized (sc) sample the pellets were dissolved in ethylene glycol by heating to 450 K and then crystallized by slow cooling.[4] The concentration was about 50 g/L and the precipitation temperature about 420 K. The gel produced was vacuum-filtered and then washed with an excess of doubly-distilled water to remove the high-boiling ethylene glycol. The thick, wet powder obtained was then ground and dehydrated over P_2O_5 in a desiccator and finally dried in a vacuum oven at 370 K to produce a fine powder. The melt-crystallized (mc) sample was produced by grinding the pellets with a commercial mill. The changes to the Nylon by this process are insignificant, as could be seen by DSC scans before and after grinding. The Nylon 6 sample (M_w of 9500 and a M_n of 14 000) was obtained from Allied-Signal Co. and was used as received in powder form. It has a T_m = 495 K and a T_g = 313 K. Crystallinities were determined by DSC from the heats of fusion and were 47% (sc Nylon 6.6), 29% (mc Nylon 6.6), and 45% (Nylon 6). The equilibrium heat of fusion for Nylon 6.6 was taken to be 57.4 kJ/mol.[15] This value should characterize the best solution-crystallized α_1 form, without pseudohexagonal content.[21] For Nylon 6 the equilibrium heat of fusion was assumed to be 26 kJ/mol.[22]

Neutron Scattering. The neutron scattering experiments were done with the QENS instrument at the Intense Pulsed Neutron Source (IPNS) at Argonne National Laboratory. The instrument covers a momentum transfer range of $0.5 < k < 2.5$ Å^{-1}, roughly corresponding to interactions at a scale less than 10 Å. The energy resolution is about 70 μeV (FWHM) at zero energy transfer (1 meV corresponds to a frequency of 2.4×10^{11} Hz and a correlation time of 4.1×10^{12} s). Details about the design and operation of QENS have been given elsewhere.[23] In all experiments a Si filter was used in the incident beam to reduce the fast neutron background. The powder samples were sealed in an aluminum tube (thickness of 1 cm and length of 10 cm) inside a drybox. For low temperatures a Displex helium refrigerator was used and for high temperatures (above room) we used a Howe furnace. The temperature control assured a ±1 K accuracy in temperature, but there was always a temperature gradient due to the length of the sample holder, being 1–2 K at low temperatures and reaching 6 K at the highest temperatures measured. Collection times were typically 10 h. For all runs a flat background was substracted to remove the contribution of electronic noise and background from the delayed neutrons coming from the enriched uranium booster target. No correction was made for multiphonon contributions as the elastic and inelastic regions were well separated. No multiple scattering corrections were made. A vanadium cylinder was run at room temperature and all intensities were then corrected for the efficiency of the detector banks on the basis of the vanadium run.

Results

The experimental results for the three samples investigated are included in Table I. Data were collected for sc Nylon 6.6 at 20, 220, 300, 400, and 500 K. A typical plot of the corrected scattering functions $S(k,\omega)$ at different temperatures and constant k = 2.41 Å^{-1} is shown in Figure 1. The spectrum at the lowest temperature, 20 K, gives the instrument resolution. Very little broadening of the elastic lines occurs at 220 K, and the curves at these temperatures can be fitted by a δ function convoluted with the resolution function. At 300 K a small Lorentzian must be convoluted with the resolution function in order to fit the data for k above 1.88 Å^{-1}. At high temperatures the Lorentzian component increases in magnitude. The increase is gradual and the effect becomes most pronounced between 400 and 500 K. At this latter temperature, still below the melting peak at 540 K, there is hardly any elastic intensity left.

For mc Nylon 6.6, data were collected at 300, 400, and 500 K. At 300 K, a very small Lorentzian component could be identified at three k settings. For the remaining six k values the data statistics were not adequate for separation of such a small Lorentzian component (see Table I).

Nylon 6 was measured at 20, 200, 300, 350, 400, and 440 K and in the melt, at 525 K. Below room temperature, no quasielastic broadening occurs, as was the case for the other two samples. At 300 K, a small Lorentzian component improves the fit of the data for some k values. At 350 K, only a small increase in intensity and width of the Lorentzian component is observed. The increase is larger, albeit still gradual, at the two highest temperatures measured. In the melt (data not included in Table I) the elastic component disappears completely for the higher k values, where the fit is the best for two Lorentzian components and no δ function.

The data on the elastic intensity are shown as a function of temperature in Figure 2a,b for sc Nylon 6.6 and Nylon 6, respectively; they have been normalized to the intensities at 20 K for each k value. Qualitatively similar results were also obtained for mc Nylon 6.6, a sample with a crystallinity lower than that of sc Nylon 6.6. The data are not shown due to the lack of a 20 K run for normalization. Below the calorimetric glass transition, the proton motion is adequately described by a Debye–Waller factor with a

Table I
Quasielastic Neutron Scattering Data for Aliphatic Nylons[a]

		k (Å^{-1})								
T (K)		0.58	0.91	1.23	1.62	1.88	2.11	2.24	2.41	2.54
Solution-Crystallized Nylon 6.6 (Crystallinity = 47%)										
20	I_T		582			616			591	
220	I_T		433			426			392	
300	I_T		367			342			307	
	EISF		1.00			0.93			0.88	
	L		–			73			58	
400	I_T		256			199			164	
	EISF		0.82			0.69			0.66	
	L		99			152			185	
500	I_T	177	169			102	84	76	79	
	EISF	0.51	0.38			0.14	0.08	0.09	0.11	
	L	116	165			344	400	479	484	
Melt-Crystallized Nylon 6.6 (Crystallinity = 29%)										
300	I_T	439	526	429	492	501	381	379	466	372
	EISF	1.00	0.96	1.00	1.00	0.92	1.00	1.00	0.89	1.00
	L	–	204	–	–	257	–	–	119	–
400	I_T		367	356	383	324			269	256
	EISF		0.81	0.75	0.70	0.64			0.58	0.56
	L		171	171	242	222			209	239
500	I_T	313	295	263	274	224	203	185	174	164
	EISF	0.73	0.60	0.50	0.42	0.33	0.29	0.27	0.27	0.24
	L	181	205	232	286	304	394	358	341	352
Nylon 6 (Crystallinity = 45%)										
20	I_T	802	986	796	829	1006	799	838	1000	812
200	I_T	596	606	580	598	592	534	552	568	535
300	I_T	475	561	498	498	496	411	380	484	433
	EISF	1.00	0.92	1.00	1.00	0.84	1.00	1.00	0.87	1.00
	L	–	53	–	–	38	–	–	56	–
350	I_T		548			466			434	
	EISF		0.88			0.81			0.81	
	L		79			72			98	
400	I_T	414	449	411	387	356	310	309	324	300
	EISF	0.88	0.83	0.78	0.74	0.70	0.70	0.72	0.71	0.72
	L	102	95	88	86	93	101	136	149	167
440	I_T	467	422	441	407	325	316	321	282	292
	EISF	0.85	0.77	0.72	0.66	0.60	0.59	0.42	0.42	0.43
	L	106	102	122	119	127	135	186	168	183

[a] I_T is total intensity corrected for the efficiency of the individual detector banks (relative units), EISF is the elastic incoherent structure factor, L is the half-width at half-maximum of the Lorentzian peak (μeV); empty spaces indicate that no experiment was done at that k setting; dashes or omitted columns indicate that no Lorentzian was needed for the fit of the data.

mean-square amplitude that varies linearly with temperature. The corresponding exponential attenuation of the intensity is indicated by solid lines in Figure 2a,b. The additional decrease, starting above T_g, must be accounted for by larger-amplitude diffusional motion.

The k dependence of the EISF for sc Nylon 6.6 at different temperatures is shown in Figure 3. At temperatures smaller than 300 K the EISF is independent of k, as expected in the absence of diffusive motion. At 400 K the fall-off in $A(k)$ is significant, reaching a value of 0.66. This decrease indicates either restricted motion of all protons or unrestricted motion of about half of the protons in Nylon 6.6. At 500 K, $A(k)$ goes almost to zero, indicating practically free motion of all protons in the time scale of the experiment.

We have modeled the k dependence of the EISF in sc Nylon 6.6, using the following assumptions: at 400 K the protons in the amorphous parts undergo continuous rotational diffusion on a sphere of radius r_a, as expressed by eq 3, and the protons in the crystalline portions undergo restricted rotational jumps between n equivalent points on a circle of radius r_c, as given by eq 2. The total EISF has been arrived at by assuming simple additive contributions from the crystalline and amorphous regions:[24]

$$A(k) = w^c A_c(k) + (1 - w^c) A_a(k) \qquad (5)$$

using the calorimetric $w_c = 0.47$. The model parameters r_a, r_c, and n were least-squares adjusted to the observed EISF's at each given temperature. The results of the model fit are shown by the solid lines in Figure 3. The distance values thus obtained at 500 K for the sc Nylon 6.6 are r_a

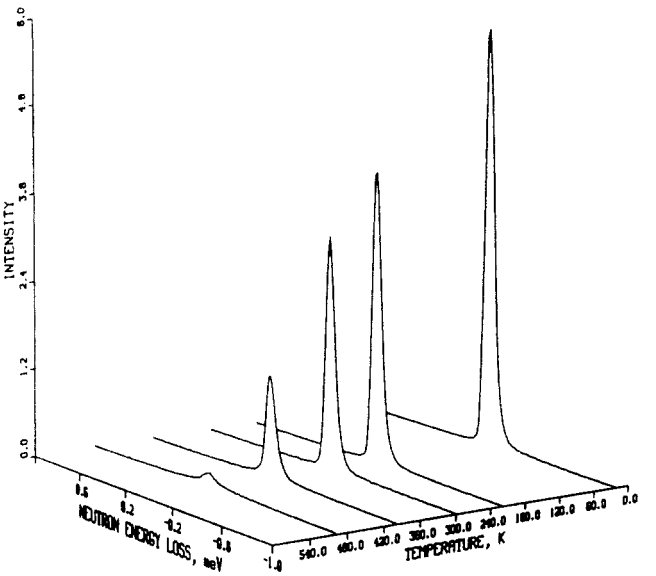

Figure 1. Neutron spectra of solution-crystallized Nylon 6.6 for a momentum transfer of 2.41 Å^{-1}. The spectrum for the highest temperature, 500 K, is typical of a liquid material.

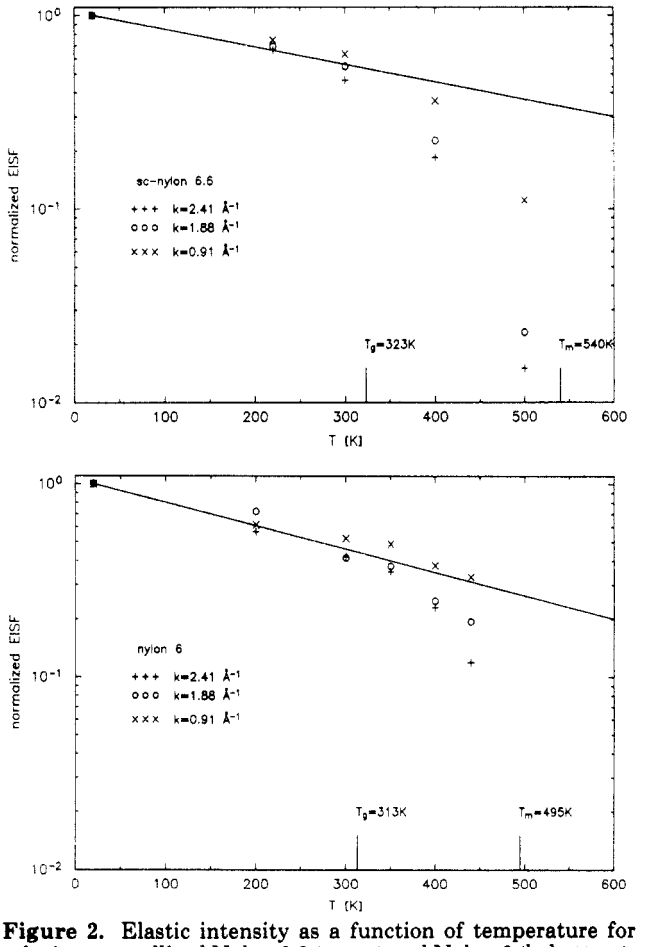

Figure 2. Elastic intensity as a function of temperature for solution-crystallized Nylon 6.6 (a, top) and Nylon 6 (b, bottom). Below T_g the motion is oscillatory, as indicated by the solid line, drawn through all points in that temperature range. An extra decrease due to diffusive motion is observed above T_g.

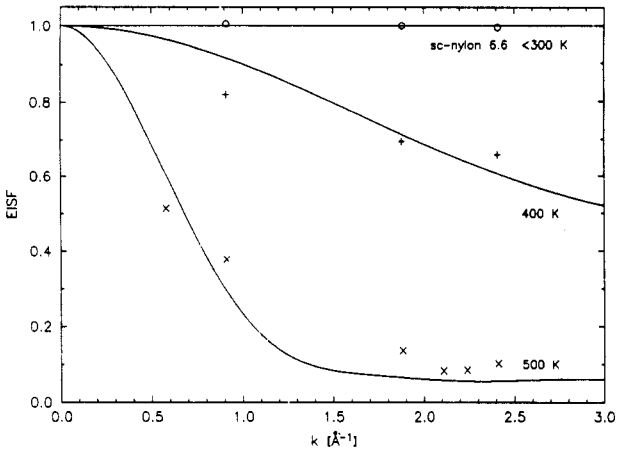

Figure 3. Elastic incoherent structure factor for solution-crystallized Nylon 6.6 as a function of momentum transfer, k, at three different temperatures. The calculated model curves are for unrestricted rotational diffusion of protons in the amorphous regions and restricted rotational diffusion of methylene groups in the crystalline regions.

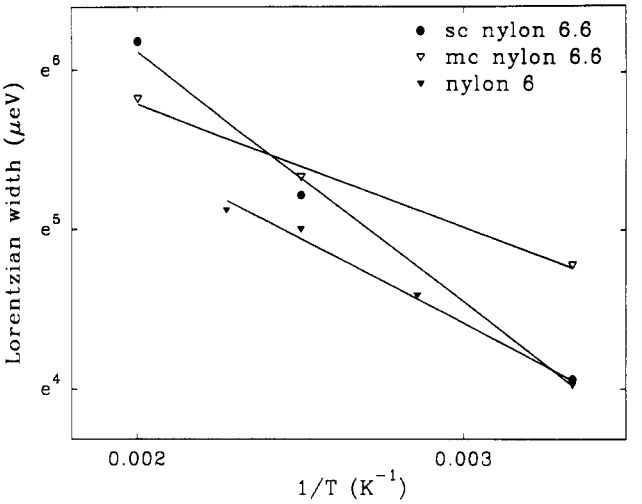

Figure 4. Lorentzian line widths as a function of temperature, for a momentum transfer of 2.41 Å^{-1}. The solid lines, drawn by assuming an Arrhenius process, indicate activation energies of 13.1, 6.5, and 8.6 kJ/mol for the sc Nylon 6.6, mc Nylon 6.6, and Nylon 6, respectively.

= 1.8 Å and r_c = 2.4 Å. A similar fit could be obtained at 500 K for the mc Nylon 6.6 with a w_c = 0.9 and a different value for r_a (0.8 Å). At 400 K, the same r_a (0.8 Å) is found for both Nylon 6.6 samples. The model chosen for the motion in the amorphous and crystalline regions requires r_a to correspond to some length related to the C–H bond, while r_c should be about half of the interchain distance for Nylon crystals. Both obtained parameters are reasonable when compared to the molecular and crystal structures. The number of equivalent points between jumps in the crystalline regions was found to be n = 1 at 400 K and n > 8 at 500 K. These model parameters suggest that the protons in the amorphous parts of Nylon 6.6 become mobile above the calorimetric T_g. The protons in the crystalline regions, in contrast, undergo only small-amplitude periodic motions about one site (a motion that can be described as libration) up to 400 K. Increasing the temperature to 500 K, the protons (and the methylene groups to which they are attached) undergo jumps on a cylinder between a large number of equivalent sites, a situation that for the neutrons is almost equivalent to unrestricted rotational diffusion.

For both Nylon 6.6 and Nylon 6, the decrease in the elastic scattering above 300 K is accompanied by quasielastic broadening, described by a single Lorentzian (eq 4). The width of this Lorentzian is inversely proportional to the time scale of the motion. The time scale of the motions appears to be similar, within the instrument resolution, in both the crystalline and amorphous portions of all Nylon samples studied, since only one Lorentzian is needed to fit the data. Values found at k = 2.41 Å^{-1} are 0.43 × 10^{-11} and 0.61 × 10^{-11} s at 500 K for sc and mc Nylon 6.6, 1.1 × 10^{-11} s at 400 K for sc Nylon 6.6, and 1.2 × 10^{-11} s for Nylon 6 at 440 K. They are of the same order of magnitude as the NMR estimate of the correlation times (10^{-11} s).[7-9] The values determined here represent average time scales, as amorphous and crystalline regions cannot be distinguished in a single experiment. A k dependence of the Lorentzian line widths simply indicates a distribution of spatial and temporal extent of the motion, as expected for a semicrystalline polymer. The line widths are approximately linearly proportional to k, while the slow segmental dynamics found in the melt, and described by a Rouse mode, would require a k^4 dependence.[25]

Figure 4 shows the temperature dependence of the Lorentzian line width for k = 2.41 Å^{-1}, with the solid lines describing an Arrhenius-type process of the form

$$\ln(\tau/\tau_0) = E_a/RT \qquad (6)$$

with E_a representing an activation energy and τ_0 a correlation time characteristic of the process (the gas constant R = 8.314 J K^{-1} mol^{-1}). The average E_a derived from a least-squares fit of eq 6 to all data, samples, and k settings is 8.6 ± 2.7 kJ/mol. The deviation reflects thus only the averaging of all values and not the uncertainty of any individual Arrhenius plot. Within the error limits of our experiments, the determined value of E_a suggests a similar mechanism of diffusive motion with a relatively low activation barrier in all the analyzed Nylons.

Discussion

The Nylons studied show an initial drop in EISF in the calorimetric glass transition region (data of Table I). This is consistent with the onset of diffusive proton motion in the amorphous portions of the materials. (The motion involved in the γ-relaxation, studied by IQNS methods for polyethylene in ref 24, is too slow for the resolution of the QENS instrument used here. All slower motions are included in the resolution peak, and thus, no quasielastic broadening is noted below room temperature.) A similar drop in intensity was seen in IQNS experiments on systems without the complication of crystallinity, specifically amorphous polybutadiene[26] and 1,2,3-tri-α-naphthylbenzene.[27] It has been interpreted by the presence of fast, local motion in the vicinity of the calorimetric T_g. The picosecond time scale diffusive motion, observed directly in the neutron scattering experiment, represents thus the basic atomic motion of the glass transition. Cooperative coupling of this motion leads to the slow macroscopic response to external stimuli. For example, the calorimetric glass transition corresponds to a cooling rate of 1–10 K/min and is usually equivalent to dynamic mechanical analysis at about 1 Hz. The atomic motion on a picosecond time scale must thus not be confused with the time scale of the calorimetric glass transition. Quite in line with this description is the activation energy of 9 kJ/mol derived here for the atomic scale motion. This low value should be compared to the apparent activation energy of hundreds of kilojoules per mole obtained through a WLF-type analysis of the glass transition.[28]

The additional drop in the normalized EISF at higher temperatures (shown in Figures 2a and 3) must reflect

motion of the methylene groups in the crystalline regions. The somewhat smaller attenuation for the lower crystallinity Nylon 6.6 sample shown in Table I was accounted for in our model by a smaller value of r_a. Overall, these results support thus the conclusion of a considerable proton mobility in the crystalline regions of the materials. In Nylon 6.6, the drop in the EISF is so large that at temperatures 40 K below melting all methylene groups must undergo large-amplitude motions in the time window of our experiment.

The results for Nylon 6 at 400 K in Figure 2b and Table I are similar to those of Nylon 6.6. At equal supercooling, however, the intensity attenuation is smaller in magnitude, and the Lorentzian line widths narrower, indicating that the spatial extent of the motions in Nylon 6 is not dependent on the thermodynamic supercooling but rather on the absolute temperature and possible small differences in the crystal structure. All three Nylon samples studied deviate substantially from the behavior of a harmonic oscillator above the glass transition, as shown in Figure 2 and in Table I. It was recently shown[29] that Nylon 6 also exhibits a Brill transition, that is more gradual and diffuse compared to the changes in Nylon 6.6. This finding supports the similar dynamics seen for Nylon 6 and Nylon 6.6 samples in this work. Similarly, the thermal analysis work has also shown that the increase in heat capacity above the glass transition temperature beyond that expected for a rigid crystal and a liquid amorphous phase is characteristic of all aliphatic Nylons.[10,11]

The motion, as determined by the IQNS experiment, should be compared with the results of other experimental methods. The X-ray data indicate a high-temperature pseudohexagonal structure,[4] implying a local hexagonal environment for the methylene groups. The neutron scattering data presented here also show the protons in the crystal sample many positions beyond the amplitude of the oscillatory motion of the chain at 500 K. This motion, suggested by the simple model of eq 2 and displayed in Figure 3, is almost equivalent to an isotropic rotational diffusion of the chain. Such motion was not believed to occur, however, given the retention of the H bonds up to the melting temperature.[6] The NMR line shape analysis indicates that the motion present at 500 K is 60° librations and not trans–gauche isomerizations.[7-9] The heat capacity increase, however, could not be explained by librations only.[11]

These initially conflicting observations can be reconciled by looking at the recent results of molecular dynamics simulations on model polyethylene and paraffin crystals.[14,30] Similar to the observation in Nylons, both paraffins and polyethylene show an increase in heat capacity, beginning typically more than 100 K below the melting temperature.[31] This increase was explained by trans–gauche isomerizations that are seen to occur continuously on a picosecond time scale, in addition to excursions of the torsional angle to values lower than 90° (i.e. librations).[32] The percentage of gauche bonds is small (1–2% up to 400 K) but sufficient to quantitatively account for the heat capacity results, as well as IR data on the gauche concentration in paraffins.[33] In addition to these gradual changes, some paraffins change to a hexagonal phase before melting. This high-temperature phase has been called a "rotor" phase, because it had been originally proposed to involve a whole-chain rotation.[34] The mobility via the trans–gauche defects (conformational defects) found in the simulations could not lead to a cylindrical symmetry, necessary for the hexagonal crystal structure. A much larger concentration of twist defects with individual bond-rotation angles of less than 90° was observed to produce a continuous reorientation of the zigzag planes of the paraffin chains in nanometer-size domains, also on a picosecond time scale. It is thus the time and position average of this domain structure that leads to the hexagonal X-ray structure. A similar mechanism may also apply to the observed pseudohexagonal phase in the Nylons. The controlling factor for the increase in heat capacity is the 1–2% concentration of conformational defects, a too low amount to be detected by NMR experiments. The controlling factor for the local hexagonal environment is the preponderance of librations found in the NMR work. Given the large amplitude of the librations and averaging over all methylene groups along the chain, the full diameter of a cylinder can be sampled by the protons, in agreement with the neutron scattering data presented here. This new insight into the structure and motion of polymers obtained from the computer simulations allows one, thus, to account for the apparent conflict of the experimental data.

Acknowledgment. We are indebted to the QENS instrument scientist Frans Trouw for invaluable help during the course of this work. Research was sponsored by the Division of Materials Sciences, Office of Basic Energy Sciences, U.S. Department of Energy, under Contract No. DE-AC05-84OR21400 with Martin Marietta Energy Systems, Inc., and by the National Science Foundation, Division of Materials Research, Grant No. DMR-88-18412. The neutron scattering experiments were performed at the IPNS at Argonne National Laboratory, where research is sponsored by the U.S. Department of Energy, BES-Materials Science, under Contract No. W-31-109-ENG-38.

References and Notes

(1) Clark, E. S.; Wilson, F. C. In *Nylon Plastics*; Kohan, M. I., Ed.; Wiley-Interscience: New York, 1973; Chapter 8.
(2) Wunderlich, B. *Macromolecular Physics*; Academic Press: New York, 1973; Vol. 1.
(3) Brill, R. *J. Prakt. Chem.* **1942**, *161*, 49.
(4) Starkweather, H. W., Jr.; Jones, G. A. *J. Polym. Sci., Polym. Phys. Ed.* **1981**, *19*, 467.
(5) Slichter, W. P. *J. Polym. Sci.* **1958**, *35*, 77.
(6) Trifan, D. S.; Terenzi, J. F. *J. Polym. Sci.* **1958**, *28*, 443.
(7) Hirschinger, J.; Miura, H.; Gardner, K. H.; English, A. D. *Macromolecules* **1990**, *23*, 2153.
(8) Miura, H.; Hirschinger, J.; English, A. D. *Macromolecules* **1990**, *23*, 2169.
(9) Wendoloski, J.; Gardner, K. H.; Hirschinger, J.; Miura, H.; English, A. D. *Science* **1990**, *247*, 431.
(10) Xenopoulos, A.; Wunderlich, B. *Polymer* **1989**, *31*, 1260.
(11) Xenopoulos, A.; Wunderlich, B. *J. Polym. Sci., Polym. Phys. Ed.* **1990**, *28*, 2271.
(12) Xenopoulos, A.; Wunderlich, B. *Colloid Polym. Sci.* **1991**, *269*, 375.
(13) Wunderlich, B.; Grebowicz, J. *Adv. Polym. Sci.* **1984**, *60/61*, 1. Wunderlich, B.; Möller, M.; Grebowicz, J.; Baur, H. *Conformational Motion and Disorder in Low and High Molecular Mass Crystals*; Advances in Polymer Science 87; Springer Verlag: Berlin, 1988.
(14) Sumpter, B. G.; Noid, D. W.; Wunderlich, B. *J. Chem. Phys.* **1990**, *93*, 6875; *Macromolecules* **1992**, *25*, 7247.
(15) Magill, J. H.; Girolamo, M.; Keller, A. *Polymer* **1981**, *22*, 43.
(16) Allen, G.; Higgins, J. S. *Rep. Prog. Phys.* **1973**, *36*, 1073.
(17) Lovesey, S. W. *Theory of Thermal Neutron Scattering*; Clarendon Press: Oxford, U.K., 1984; Vol. 1.
(18) Bée, M. *Quasielastic Neutron Scattering*; Adam Hilger: Bristol, PA, 1988.
(19) Barnes, J. D. *J. Chem. Phys.* **1973**, *58*, 5193.
(20) See papers in: *Polymer Motion in Dense Systems*; Richter, D., Springer, T., Eds.; Springer Proceedings in Physics 29; Springer Verlag: Berlin, 1988.
(21) Illers, K.-H. *Progr. Colloid Polym. Sci.* **1975**, *58*, 61.

(22) Illers, K.-H. *Makromol. Chem.* **1978**, *179*, 497. Wunderlich, B. *Macromolecular Physics*; Academic Press: New York, 1980; Vol. 3.
(23) Bradley, K. F.; Chen, S.-H.; Brun, T. O.; Kleb, R.; Loomis, W. A.; Newsam, J. M. *Nucl. Instrum. Methods Phys. Res.* **1988**, *A270*, 78.
(24) Peterlin-Neumaier, T.; Springer, T. *J. Polym. Sci., Polym. Phys. Ed.* **1976**, *14*, 1351.
(25) Allen, G.; Higgins, J. S.; Maconnachie, A.; Ghosh, R. E. *J. Chem. Soc., Faraday Trans. 2*, **1982**, *78*, 2117.
(26) Frick, B. *Prog. Colloid Polym. Sci.* **1989**, *80*, 164.
(27) Fujara, F.; Petry, W. In ref 20, p 149.
(28) McCrum, N. G.; Read, B. E.; Williams, G. *Anelastic and Dielectric Effects in Polymeric Solids*; Wiley: London, 1967.
(29) Murthy, N. S.; Curran, S. A.; Aharoni, S. M.; Minor, H. *Macromolecules* **1991**, *24*, 3215.
(30) Liang, G.; Noid, D. W.; Sumpter, D. W.; Wunderlich, B. *Macromolecules*, submitted for publication.
(31) Jin, Y.; Wunderlich, B. *J. Phys. Chem.* **1991**, *95*, 9000.
(32) Noid, D. W.; Sumpter, B. G.; Varma-Nair, M.; Wunderlich, B. *Makromol. Chem., Rapid Commun.* **1989**, *10*, 377.
(33) Kim, Y.; Strauss, H. L.; Snyder, R. G. *J. Phys. Chem.* **1989**, *93*, 7520.
(34) Müller, A. *Proc. R. Soc. London* **1932**, A138, 514.